Molecular Medicine

Transgenic Expression of miR-222 Disrupts Intestinal Epithelial Regeneration by Targeting Multiple Genes Including Frizzled-7

Hee Kyoung Chung,[1,2] Yu Chen,[1,2] Jaladanki N Rao,[1,2] Lan Liu,[1,2] Lan Xiao,[1,2] Douglas J Turner,[1,2] Peixin Yang,[3] Myriam Gorospe,[4] and Jian-Ying Wang[1,2,5]*

[1]Cell Biology Group, Department of Surgery, University of Maryland School of Medicine, Baltimore, Maryland, United States of America; [2]Baltimore Veterans Affairs Medical Center, Baltimore, Maryland, United States of America; [3]Department of Obstetrics, Gynecology, and Reproductive Sciences, University of Maryland School of Medicine, Baltimore, Maryland, United States of America; [4]Laboratory of Genetics, National Institute on Aging (NIA)–Intramural Research Program (IRP), National Institutes of Health, Baltimore, Maryland, United States of America; [5]Department of Pathology, University of Maryland School of Medicine, Baltimore, Maryland, United States of America; and *current address: Department of Digestive Diseases, Xijing Hospital, Fourth Military Medical University, Xi'an, PR China

Defects in intestinal epithelial integrity occur commonly in various pathologies. miR-222 is implicated in many aspects of cellular function and plays an important role in several diseases, but its exact biological function in the intestinal epithelium is underexplored. We generated mice with intestinal epithelial tissue-specific overexpression of miR-222 to investigate the function of miR-222 in intestinal physiology and diseases *in vivo*. Transgenic expression of miR-222 inhibited mucosal growth and increased susceptibility to apoptosis in the small intestine, thus leading to mucosal atrophy. The miR-222–elevated intestinal epithelium was vulnerable to pathological stress, since local overexpression of miR-222 not only delayed mucosal repair after ischemia/reperfusion-induced injury, but also exacerbated gut barrier dysfunction induced by exposure to cecal ligation and puncture. miR-222 overexpression also decreased expression of the Wnt receptor Frizzled-7 (FZD7), cyclin-dependent kinase 4 and tight junctions in the mucosal tissue. Mechanistically, we identified the *Fzd7* messenger ribonucleic acid (mRNA) as a novel target of miR-222 and found that (miR-222/*Fzd7* mRNA) association repressed *Fzd7* mRNA translation. These results implicate miR-222 as a negative regulator of normal intestinal epithelial regeneration and protection by downregulating expression of multiple genes including the *Fzd7*. Our findings also suggest a novel role of increased miR-222 in the pathogenesis of mucosal growth inhibition, delayed healing and barrier dysfunction.

Online address: http://www.molmed.org
doi: 10.2119/molmed.2015.00147

INTRODUCTION

The mammalian intestinal epithelium is in a constant state of renewal, characterized by active proliferation of stem cells localized near the base of the crypts and progression of these cells up the crypt-villus axis with cessation of proliferation and subsequent differentiation and apoptosis (1,2). The epithelium of the human small intestine undergoes ~10^{11} mitoses per day, and this dynamic turnover rate is tightly regulated by numerous factors at multiple levels (1–3). In response to stressful environments, the successful repair of damaged mucosa and maintenance of the intestinal epithelial integrity require epithelial cell decisions that regulate signaling networks controlling expression of various genes involved in cell survival, apoptosis, migration and proliferation (2,3). Disruption of the intestinal epithelial integrity occurs commonly during critical surgical conditions, leading to the translocation of luminal toxic substances and bacteria to the bloodstream and in some instances multiple organ dysfunction syndrome and death (4,5). However, the exact mechanism by which the intestinal epithelial integrity is preserved under biological and pathological conditions remains largely unknown.

Micro–ribonucleic acids (miRNAs) are small noncoding RNAs that bind to specific mRNAs and inhibit translation and/or promote mRNA degradation (6,7). High-throughput and functional studies show that miRNAs play impor-

Address correspondence to *Jian-Ying Wang, Baltimore Veterans Affairs Medical Center (112), 10 North Greene Street, Baltimore, MD 21201. Phone: 410-605-7000, ext. 5678; Fax: 410-605-7919; E-mail: jwang@smail.umaryland.edu.*
Submitted June 12, 2015; Accepted for publication July 30, 2015; Published Online (www.molmed.org) August 3, 2015.

tant roles in physiological and pathological processes (6,8,9). Recently, miRNAs have emerged as master regulators of the gut epithelial homeostasis (3,10,11). We have profiled global miRNA expression in cultured intestinal epithelial cells (IECs) (2) and intestinal mucosa in mice (13) and have found that several miRNAs, including miRNA-222, miRNA-29b, miRNA-322/503 and miR-195, are highly expressed in the intestinal epithelium, and their expression levels are affected rapidly in response to food starvation and polyamine depletion. Further studies show that control of the expression of these miRNAs is crucial for maintenance of normal intestinal epithelial integrity and plays an important role in mucosal pathology. For example, mucosal atrophy in fasted mice is associated with increased miR-29b, whereas miR-29 silencing by systemic delivery of locked nucleic acid–modified anti–miR-29b oligonucleotides promotes the mucosal growth (13). Moreover, miR-322/503 regulates IEC apoptosis (14), and miR-195 represses rapid epithelial restitution after wounding (15).

miR-222 (also referred as miR-222-3p) is highly conserved among different species and is clustered with miR-221 in tandem on the X chromosome (16). miR-222 modulates distinct cellular functions (17–19), and its role in cancer development can be either tumor suppressive or oncogenic, depending on cellular content and tumor type (20,21). miR-222 in human colorectal cancer cells acts in a positive feedback loop to increase expression levels of RelA and STAT3 (22), but miR-222 is a potential repressor of estrogen receptor (ER)-α expression in 3T3-L1 adipocytes (23). Our previous studies indicate that miR-222 and the RNA-binding protein (RBP) CUGBP1/CELF1 (CUG triplet repeat, RNA binding protein 1/CUGBP Elav-like member 1) synergistically inhibit cyclin-dependent kinase 4 (CDK4) translation in normal IECs by recruiting the *Cdk4* mRNA to processing bodies (12). Because most of our knowledge about miR-222 functions comes from studies conducted in cultured cells, the exact *in vivo* functions of miR-222, particularly in the intestinal epithelium, is not well understood. Here we developed transgenic mice that specially overexpress miR-222 in the intestinal epithelium and demonstrate that tissue-specific overexpression of miR-222 reduces growth and survival of the small intestinal mucosa by targeting multiple genes, including the Wnt receptor Frizzled-7 (Fzd7).

MATERIALS AND METHODS

Generation of miR222-Tg Mice

To generate miR-222 transgenic (miR222-Tg) mice, a 770–base pair (bp) fragment, including the mouse *miR-222* locus on chromosome X (289-bp primary miR-222 sequence) and human β-globin intron (222-bp 5′ upstream sequence and 259-bp 3′ sequence), was cloned into the pIRES-AcGFP1-Nuc vector (Supplementary Figure S1) by using an miR-222 cloning primer set (Supplementary Table S1). The A33 promoter was used to drive intestinal epithelial tissue-specific overexpression of the genomic miR-222 precursor, as reported by others (24,25). Transgenic founders on a pure C57BL/6J background were established by pronuclear injection at the University of Maryland, Baltimore transgenic animal core. Genotyping was performed by polymerase chain reaction (PCR) in deoxyribonucleic acid (DNA) extracted by tail clippings to identify the first generation of recombinant mice with miR222/green flourescence protein (GFP) bicistronic RNA (Supplementary Figure S2). Two founders were obtained, and they were further characterized for the transmission or the expression of the transgene. Transgenic colonies were subsequently established. Male miR-222-Tg mice mated with wild-type (WT) female mice to generate miR-222-Tg mice and their WT littermates for experiments. Representative results from two independent founders are reported here and compared with those obtained from littermate controls.

Animal Experiments

All experiments were approved according to animal experimental ethics committee guidelines by the University of Maryland Baltimore Institutional Animal Care and Use Committee. Mice were housed and handled in a specific pathogen-free breeding barrier and cared for by trained technicians and veterinarians. To examine gut mucosal growth, bromodeoxyuridine (BrdU) was incorporated in intestinal mucosa by intraperitoneal injection of 2 mg BrdU (Sigma-Aldrich) in phosphate-buffered saline. A 4-cm small intestinal segment taken from 0.5 cm distal to the ligament of Trietz and the segment of middle colon were collected 1 h after injection. To generate intestinal ischemia/reperfusion (I/R)-induced injury, mice were exposed to 30-min superior mesenteric artery ischemia, followed by 2-h reperfusion (26). Sham operation for controls involved laparotomy without mesenteric ischemia. Cecal ligation and puncture (CLP) was induced as described previously (28). The ligated cecum was punctured with a 25-gauge needle and slightly compressed with an applicator until a small amount of stool appeared. In sham-operated animals, the cecum was manipulated but without ligation and puncture. In experiments with apoptosis, mice were injected (intraperitoneally) with tumor necrosis factor (TNF)-α at the dose of 25 μg/kg body weight, and the mucosal tissues were harvested for measurement of apoptotic cell death at 5 h after injection.

Histological Analysis

Dissected and opened intestines were mounted onto a solid surface and fixed in formalin and paraffin. Sections at 5 μm were stained with hematoxylin and eosin (H&E) for general histology. Slides were examined in a blinded fashion by coding them, and only after examination was complete were they decoded. By using a grade micrometer eyepiece, the overall length of villus and crypts of each section was measured, and the villus:crypt ratio was calculated. Microscopic damages in the intestinal mucosa were measured and semiquantified as described previously (27).

Assays of Gut Permeability *In Vivo*

Fluorescein isothiocyanate (FITC)-conjugated dextran dissolved in water (Sigma-Aldrich; 4KD, 600 mg/kg) was administered to mice via gavage as described (28,33). Blood was collected 4 h thereafter via cardiac puncture. The serum concentration of the FITC-dextran was determined by using a plate reader with an excitation wavelength at 490 nm and an emission wavelength of 530 nm. The concentration of FITC-dextran in sera was determined by comparison to the FITC-dextran standard curve.

Chemicals and Cell Cultures

Tissue culture medium and dialyzed fetal bovine serum were from Invitrogen, and biochemicals were from Sigma-Aldrich. The antibodies recognizing CDK4, proliferating cell nuclear antigen (PCNA), claudin-1, zona occludens-1 (ZO-1), occludin and glyceraldehyde-3-phosphate dehydrogenase (GAPDH) were obtained from Santa Cruz Biotechnology and BD Biosciences, and the secondary antibody conjugated to horseradish peroxidase was from Sigma-Aldrich. Pre-miR™ miRNA precursor and Anti-miR™ miRNA inhibitor of miR-222 were purchased from Ambion. Biotin-labeled miRNA-222 was custom-made by Dharmacon. The IEC-6 cells, stable Wnt5a-transfected fibroblasts (Wnt5a-Fs) and control fibroblasts (Con-Fs) were purchased from ATCC. IEC-6 cells were derived from normal rat intestinal crypt cells, and fibroblasts were originally isolated from mouse subcutaneous connective tissues. To establish the coculture model, stable Wnt5a-Fs or Con-Fs were precultured on the dishes for 24 h and then cocultured with IEC-6 cells for additional 4 d before wounding as described (29).

Plasmid Construction

The fragments of *Fzd7* coding region (CR) and 3′-untranslated region (UTR) were subcloned into the pmirGLO Dual-Luciferase miRNA Target Expression Vector (Promega) to generate the pmirGLO-Luc-Fzd7-CR and pmirGLO-Luc-Fzd7-3′-UTR reporter constructs as described previously (12,33). All of the primer sequences for generating these constructs are provided in Supplementary Table S1. The pMyc-TA-luciferase reporter plasmid was purchased from Addgene. Transient transfections were performed by using the Lipofectamine Reagent as recommended by the manufacturer, and the levels of firefly luciferase activity were normalized to Renilla luciferase activity.

Western Blot Analysis

Whole-cell lysates were prepared by using 2% sodium dodecyl sulfate (SDS), sonicated and centrifuged at 4°C for 15 min. The supernatants were boiled and size-fractionated by SDS–polyacrylamide gel electrophoresis (PAGE). After the blots were incubated with primary antibody and then secondary antibodies, immunocomplexes were developed by using chemiluminescence.

Reverse Transcriptase (RT)-PCR and Real-time Quantitative PCR Analysis

Total RNA was isolated by using an RNeasy mini kit (Qiagen) and used in reverse transcription and PCR amplification reactions as described (15). The levels of the *Gapdh* PCR product were assessed to monitor the evenness in RNA input in RT-PCR samples. Real-time quantitative PCR (Q-PCR) analysis was performed by using the 7500-Fast Real-Time PCR Systems with specific primers, probes and software (Applied Biosystems). For miRNA studies, the levels of miRNA-222 were also quantified by Q-PCR by using Taqman MicroRNA assay; small nuclear RNA (snRNA) U6 was used as the endogenous control.

Biotin Labeled miR-222 Pulldown Assays

Biotin-labeled miR-222 was transfected, and 24 h later, whole-cell lysates were collected, mixed with Dynabead M-280 Streptavidin beads (Invitrogen) and incubated at 4°C with rotation overnight (13). After the beads were washed thoroughly, the bead-bound RNA was isolated and subjected for RT, followed by Q-PCR analysis. Input RNA was extracted and served as control.

Assays of Newly Translated Protein and Polysome Analysis

New synthesis of nascent FZD7 protein was detected by a Click-iT protein analysis detection kit (Life Technologies) and performed following the company's manual. Briefly, cells were incubated in methionine-free medium and then exposed to L-azidohomoalanine (AHA). After mixing cell lysates with the reaction buffer for 20 min, the biotin-alkyne/azide-modified protein complex was pulled down by using paramagnetic streptavidin-conjugated Dynabeads. The pull-down material was resolved by 10% SDS-PAGE and analyzed by Western immunoblotting analysis using antibodies against or GAPDH.

Polysome analysis was performed as described (14). Briefly, cells at ~70% confluence were incubated in 0.1 mg/mL cycloheximide and then lifted by scraping in polysome extraction buffer (PEB) lysis buffer. Nuclei were pelleted, and the resulting supernatant was centrifuged through a 10–50% linear sucrose gradient to fractionate cytoplasmic components according to their molecular weights. The eluted fractions were prepared with a fraction collector (Brandel), and their quality was monitored at 254 nm by using a UV-6 detector (ISCO). After RNA in each fraction was extracted, the levels of each individual mRNA were quantified by Q-PCR in each of the fractions.

Measurement of Epithelial Repair *In Vitro*

Epithelial injury model and repair assays were carried out as described previously (29). Cells were plated at $6.25 \times 10^4/cm^2$ in Dulbecco modified Eagle medium containing fetal bovine serum on 60-mm dishes thinly coated with Matrigel according to the manufacturer's instructions (BD Biosciences) and were incubated as described for stock cultures. Cells were fed on d 2, and monolayer was wounded by removing part of

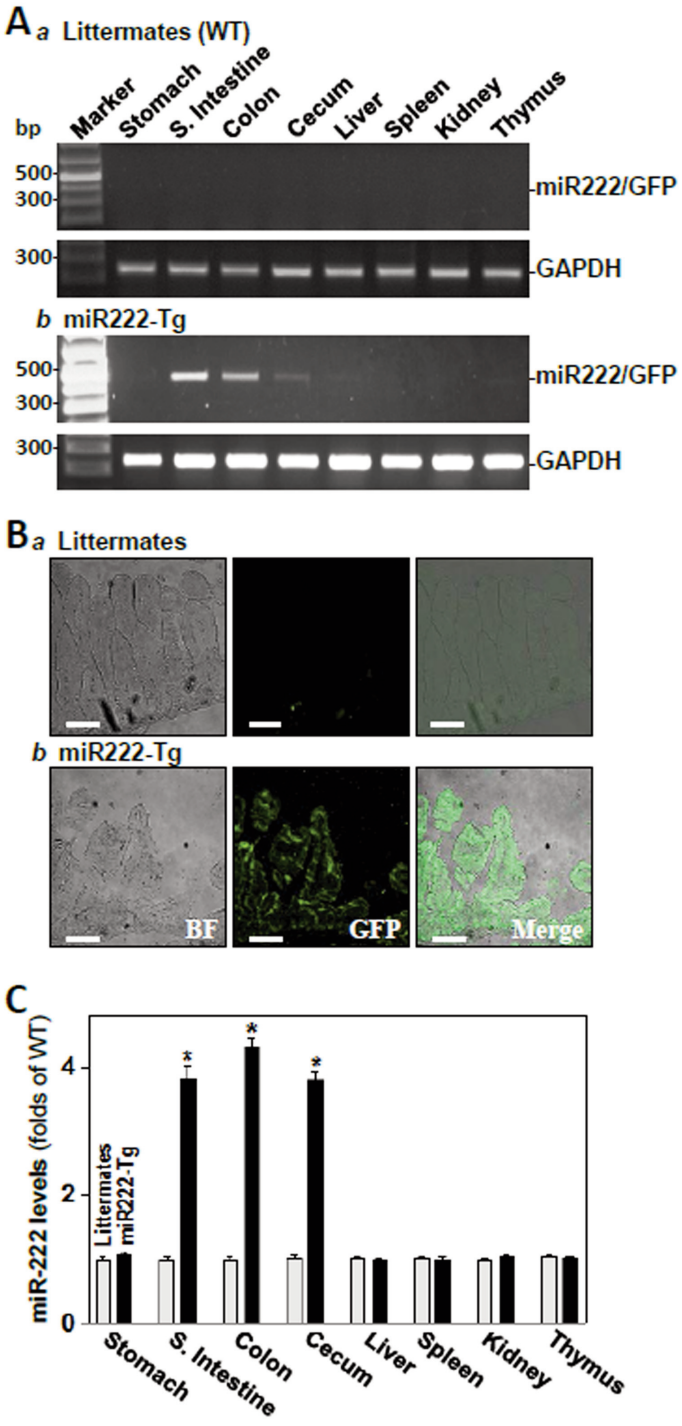

Figure 1. Characterization of miR222-Tg mice. (A) Expression of the miR-222/GFP bicistronic RNA as detected by RT-PCR in the mucosa of stomach, small (S) intestine, colon, cecum, liver, spleen, kidney and thymus of 8-wk-old littermate (a) and miR222-Tg mice (b). Total RNA was isolated and used in RT reactions. RT-PCR products of miR222/GFP were visualized in ethidium bromide–stained agarose gels; low-level amplification of GAPDH served as controls. (B) *In situ* detection of miR-222/GFP using anti-GFP antibody in the small intestine. Scale bar: 50 μm. (C) Levels of miR-222 in various tissues as measured by Q-PCR analysis. Values are means ± SEM of data from five animals. **P* < 0.05 compared with littermates.

the monolayer on d 4; repair was assayed at various times after wounding by using National Institutes of Health image analysis. All experiments were carried out in triplicate, and the results were reported as the percent of wound width covered.

Statistical Analysis

All values were expressed as the means ± standard error of the mean (SEM). An unpaired, two-tailed Student *t* test was used when indicated with $P < 0.05$ considered significant. When assessing multiple groups, one-way analysis of variance was used with the Tukey *post hoc* test. The statistical software used was SPSS17.1.

All supplementary materials are available online at www.molmed.org.

RESULTS

Transgenic Expression of miR-222 in IECs Represses Growth of Small Intestinal Mucosa

To define the *in vivo* function of miR-222 in intestinal epithelium, we used a gain-of-function transgenic approach and generated miR222-Tg mice. Age-matched miR222-Tg mice and littermate controls (3 or 4 months old) were used for comparison of phenotype. As shown, miR222-Tg mice exhibited a specific overexpression of miR222/GFP bicistronic RNA in the mucosal tissues of the small intestine, colon and cecum but not in stomach mucosa, liver, spleen, kidney and thymus, as measured by RT-PCR analysis (Figure 1A) and *in situ* detection using anti-GFP antibody (Figure 1B, Supplementary Figure S3). Consistently, miR-222 levels in miR222-Tg mice were increased by 3.9-fold, 4.3-fold and 3.8-fold in small intestine, colon and cecum, respectively, when compared with those observed in control littermates (Figure 1C). On the other hand, there were no significant changes in levels of miR-222 in stomach mucosa, liver, spleen, kidney and thymus in miR222-Tg mice compared with littermates. Because primary miR-222 also provides another form of mature miRNA (miR-222-5p), we exam-

ined changes in the levels of miR-222-5p in different tissues and demonstrated that its expression pattern was similar to that of miR-222 in miR222-Tg mice (data not shown). These results indicate that miR222-Tg mouse is a suitable transgenic model of miR-222 overexpression in the intestinal epithelium.

miR222-Tg mice looked normal in general; there were no significant differences in body weight (Figure 2A), gastrointestinal gross morphology (Figure 2B), fertility and general appearance between miR222-Tg mice and littermate controls. The first significant phenotype observed in miR222-Tg mice is that the miR-222–elevated epithelium exhibited inhibited mucosal growth in the small intestine, as evidenced by a decrease in the lengths of villi and crypts (Figures 2C, D). Abnormal histological features of the small mucosa were also observed in miR222-Tg mice, as shown by disrupted crypt structure and increased proliferation of connective tissue in the crypt area. The proliferating crypt cell population, marked by BrdU (S-phase), decreased remarkably in the small intestine of miR222-Tg mice compared with that from littermates (Figure 2E). Accordingly, the levels of cell proliferation marker proteins, PCNA and CDK4 (known target of miR-222) (12), in the small intestinal mucosa were also decreased in miR222-Tg mice (Figure 2F). We also examined changes in colonic mucosal growth in miR222-Tg mice and found that increased miR-222 did not alter mucosal growth in the colon. There were no significant decreases in the lengths of crypts and BrdU-labeled cell proliferation in miR222-Tg mice compared with littermate controls (data not shown).

Transgenic expression of miR-222 did not directly induce apoptosis in the intestinal epithelium, since there was no significant cell death observed in miR222-Tg mice as examined by transferase-mediated dUTP nick-end labeling (TUNEL) staining (Supplementary Figure S4Aa). To determine the susceptibility of intestinal epithelium to induced apoptosis, littermates and miR222-Tg mice were exposed to TNFα for 5 h. As shown, typical morphological features characteristic of apoptotic cell death were induced in the intestinal mucosa in both littermate controls and miR222-Tg mice: increased levels of TUNEL-positive cells and active caspase-3 (Supplementary Figures S4Ab, B, C).

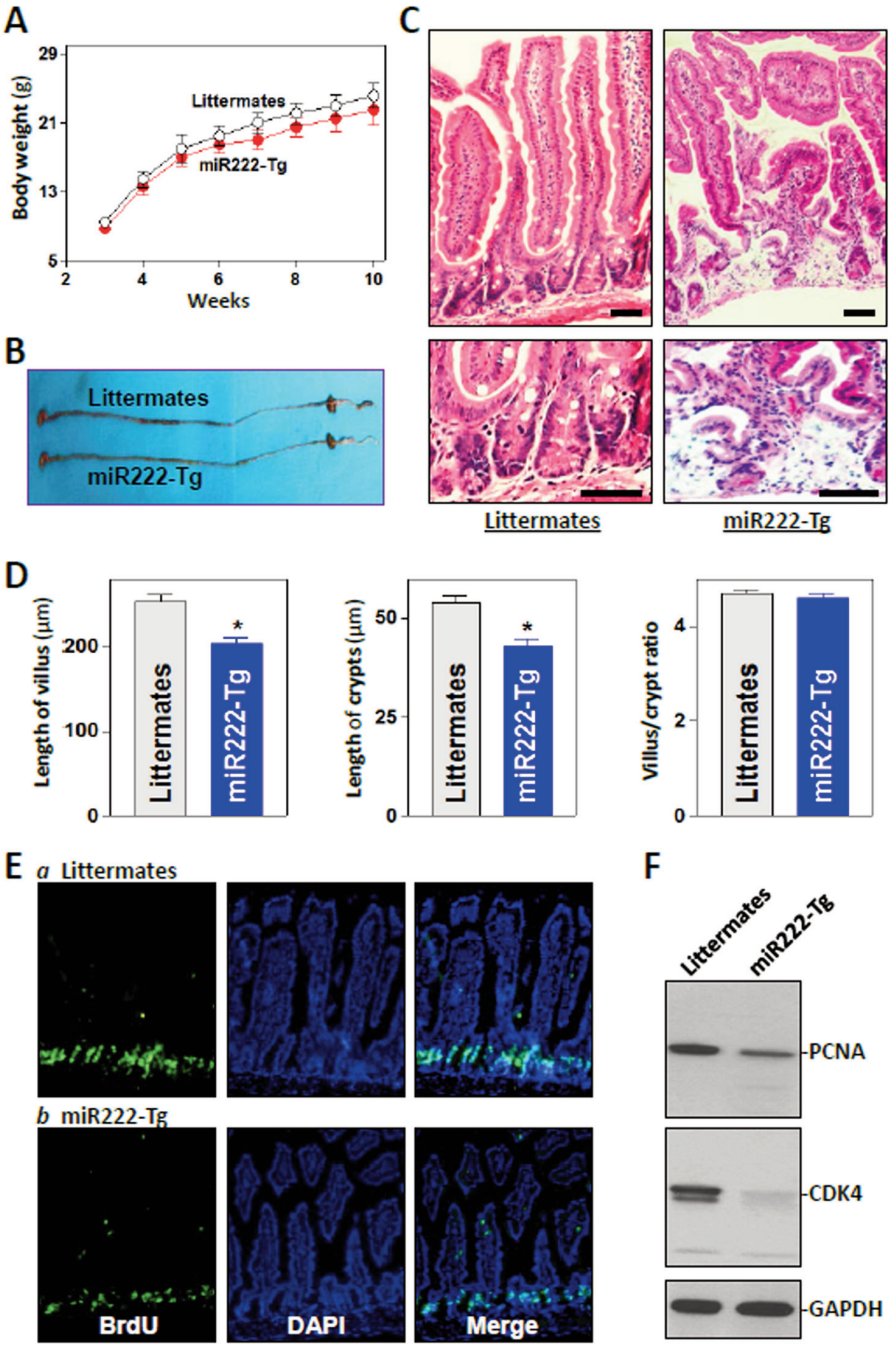

Figure 2. miR-222 inhibits growth of small intestinal mucosa. (A) Body weights in littermates and miR222-Tg mice. Values are the mean ± SEM (n = 10). (B) Gastrointestinal gross morphology. (C) Photomicrographs of the small intestine. Scale bar: 50 μm. (D) Changes in the length of villi (left), crypt (middle) and villus:crypt ratio (n = 6). *$P < 0.05$ compared with littermates. (E) Proliferating cells in small intestinal crypts as measured by BrdU labeling (1 h postinjection, green). (F) Immunoblots of PCNA and CDK4 in the mucosa.

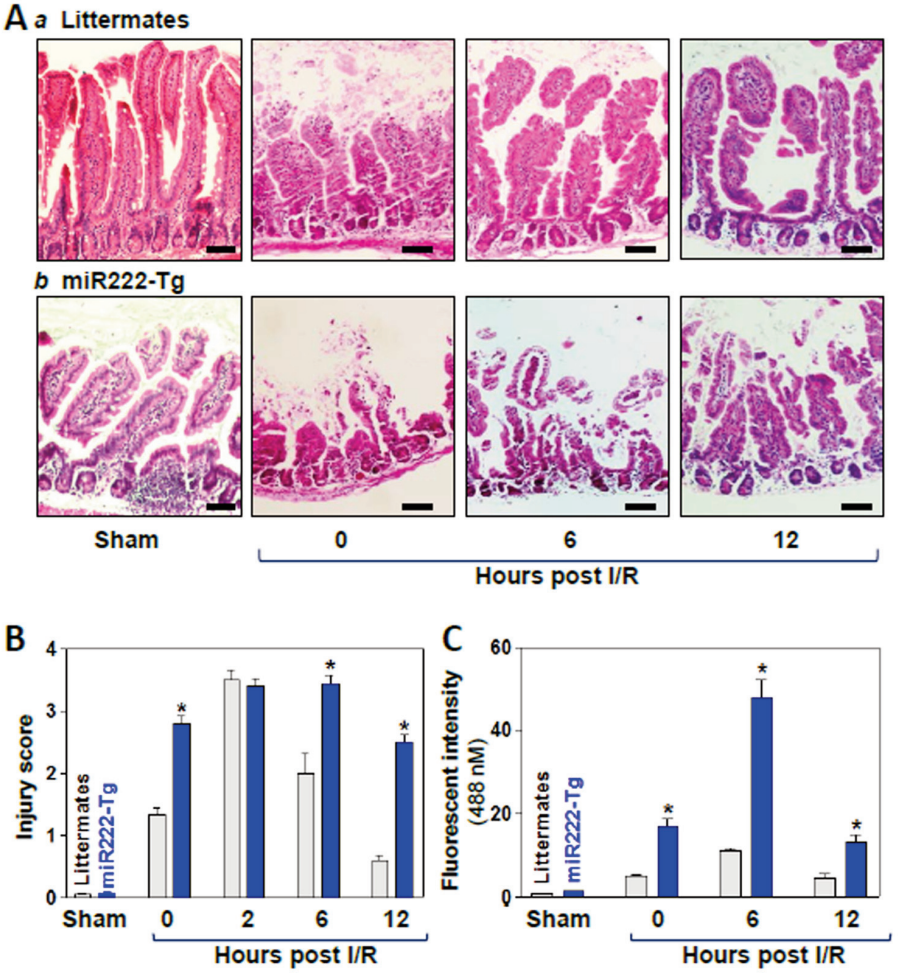

Figure 3. miR-222 delays mucosal repair of intestinal I/R-induced injury. (A) Micrographs from the intestinal mucosa of sham and I/R mice. Scale bar: 50 μm. (B) Quantification of the mucosal injury data in mice described in (A). Values are the mean ± SEM of data from five mice. *$P < 0.05$ compared with littermates. (C) Changes in gut permeability. FITC dextran was given orally, and blood samples were collected 4 h thereafter for measurement.

However, miR222-Tg mice exhibited increased percentages of apoptotic cells and more active caspase-3 compared with those observed in littermates after treatment with TNFα. These results indicate that local overexpression of miR-222 in the epithelium causes small intestinal mucosal atrophy by repressing IEC proliferation and increasing sensitivity to apoptosis.

MiR-222–Overexpressing Intestinal Epithelium Is Vulnerable to Pathological Stress

To determine if transgenic expression of miR-222 altered mucosal injury and repair after exposure to stress, the I/R model was used in this study. As expected, the mucosa of both littermates and miR222-Tg mice subjected to mesenteric I/R displayed signs of significant mucosal damage in the small intestine (Figures 3Aa and b, two middle panels in both a and b). Macroscopically, the mucosal tissue exhibited swollen and edematous with areas of red streaks. Microscopic analysis showed that there were severe sloughed cells, denuded villi with dilated capillaries and frank hemorrhage. However, tissue-specific overexpression of miR-222 in IECs enhanced mucosal injury, since the injury scores increased significantly in miR222-Tg mice compared with littermates when measured immediately after I/R (Figure 3A [second panels from left)] and Figure 3B). Increased miR-222 also delayed the process of mucosal repair after injury. The mucosa recovered quickly in littermates, as evidenced by a decrease in the injury scores at 6 and 12 h after I/R. In contrast, there was no significant repair of damaged mucosa at the same times after I/R in miR222-Tg mice, and the mucosal surface remained discontinuous, showing sloughed cells and debris (Figures 3A, B, two panels on right). Consistently, gut permeability to FITC-dextran increased in both littermates and miR222-Tg mice after I/R, but the degree of increased gut permeability in miR222-Tg mice was much higher than that observed in littermates (Figure 3C). Moreover, the recovery of the gut barrier function was slow in miR222-Tg mice compared with control littermates after I/R.

To further assess the role of increased miR-222 in the regulation of gut barrier function, we examined changes in gut permeability and expression of tight junction (TJ) proteins after CLP-induced sepsis (28). CLP stress for 24 h resulted in an acute gut barrier dysfunction in both littermates and miR222-Tg mice, as evidenced by an increase in gut permeability to FITC-dextran (Figure 4A). Like the observations in I/R model, CLP-induced gut barrier dysfunction was much more severe in miR222-Tg mice, with a decrease in the survival rate (Figure 4B). Figure 4C further showed that CLP for 24 h decreased the levels of TJ proteins, including claudin-1, ZO-1 and occludin, in the small intestinal mucosa in both littermates and miR222-Tg mice. However, the expression levels of these TJ proteins in miR222-Tg mice were much lower than those observed in littermates after exposure to CLP. Claudin-1 and ZO-1 were reduced by 55% and 80% in littermates after CLP, but their levels were decreased by 90% and >95% in miR222-Tg mice (Figure 4D), respectively, although there were no significant differences in

reduced levels of occludin proteins between littermates and miR222-Tg mice. These results indicate that locally increased levels of miR-222 enhance the vulnerability of the intestinal epithelium to I/R- and CLP-induced injury.

MiR-222 Interacts with and Represses Fzd7 mRNA Translation

The miR-222–overexpressing intestinal epithelium was associated with a dramatically decreased level of FZD7 protein (Figure 5A), although there was no change in *Fzd7* mRNA (Figure 5B). Elevated miR-222 in the epithelium did not alter the expression levels of FZD1 and FZD8, suggesting that the *Fzd7* mRNA, rather than *Fzd1* and *Fzd8* mRNAs, is a potential target of miR-222. Moreover, the levels of cyclin D1 (a downstream target of Wnt signaling) also decreased significantly in the miR-222–overexpressing epithelium compared with those observed in littermates (data not shown). Using the program RNA22, we found that there are two computationally predicted binding sites of miR-222 within the CR of the *Fzd7* mRNA (Figure 5C). To test the association of miR-222 with the *Fzd7* mRNA, RNA pull-down assay using biotin-labeled miR-222 was used in this study. As shown, cells transfected with the biotin-labeled miR-222 exhibited elevated miR-222 levels but displayed no changes in *U6* RNA levels (Figure 5D). The levels of *Fzd7* mRNA were highly enriched in the pulldown materials from cells transfected with the biotin-labeled miR-222 but not from cells transfected with a scrambled control oligomer (Figure 5E). The interaction of miR-222 with the *Fzd7* mRNA is relatively specific, because biotin–miR-222 failed to pull down the *Cdk2*, *JunD* and *Myc* mRNAs.

Furthermore, increasing the levels of cellular miR-222 (Figure 6A) by transfection with the miR-222 precursor (pre-miR-222) decreased FZD7 protein abundance (Figure 6Ba) without affecting *Fzd7* mRNA levels (Figure 6Bb). To determine if miR-222 inhibited FZD7 expression at the translation level, results in Figure 6C showed that newly synthe-

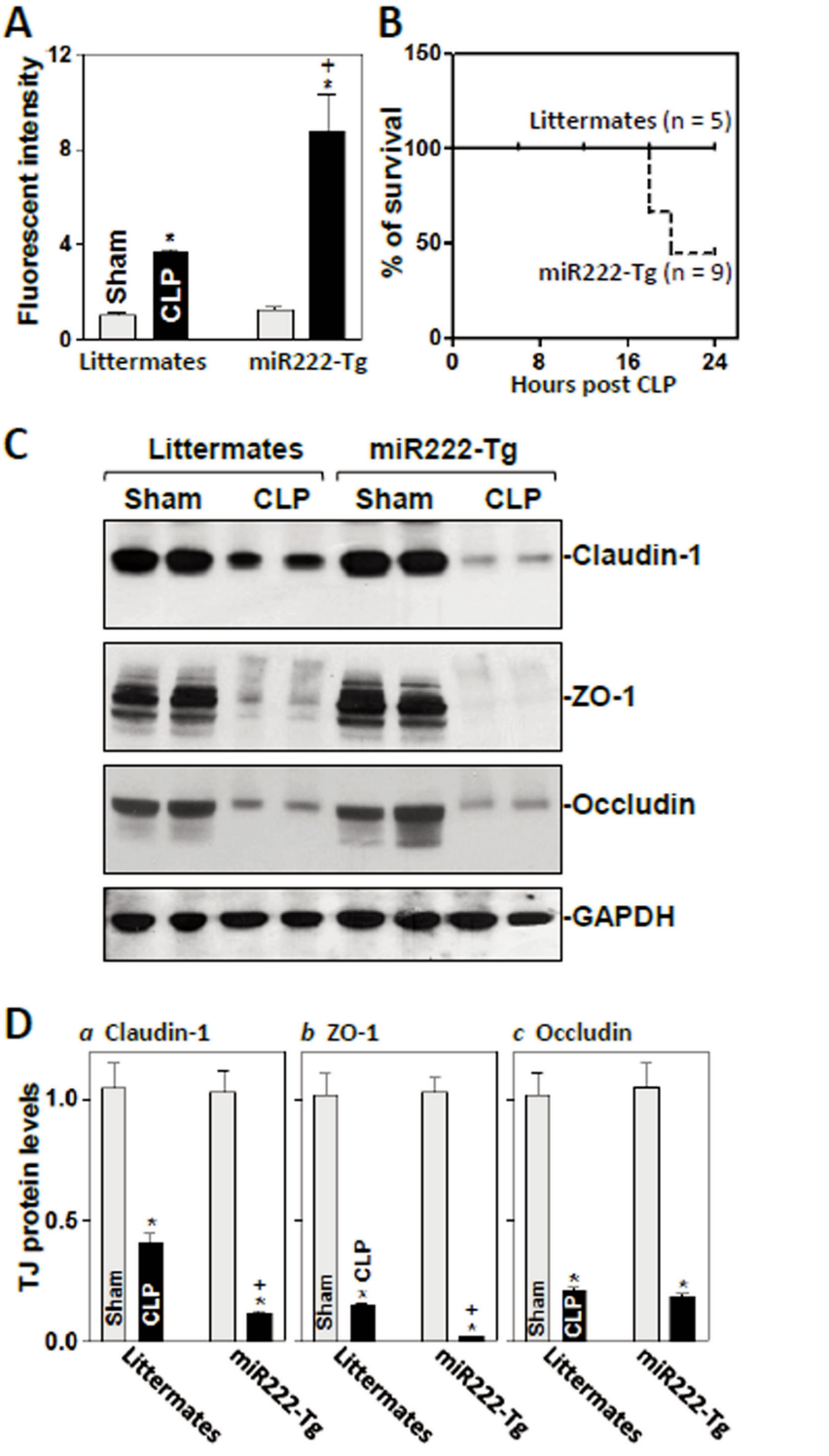

Figure 4. miR-222 aggravates gut barrier dysfunction in mice exposed to CLP. (A) Changes in gut permeability 24 h after CLP. Values are mean ± SEM of data from five animals. $^{*,+}P < 0.05$ compared with sham and littermates exposed to CLP, respectively. (B) Survival rates. (C) Immunoblots of claudin-1, ZO-1 and occludin proteins in the small intestinal mucosa described in (A). The results in each panel were from one individual animal. (D) Quantitative analysis of the immunoblots as densitometry (n = 5).

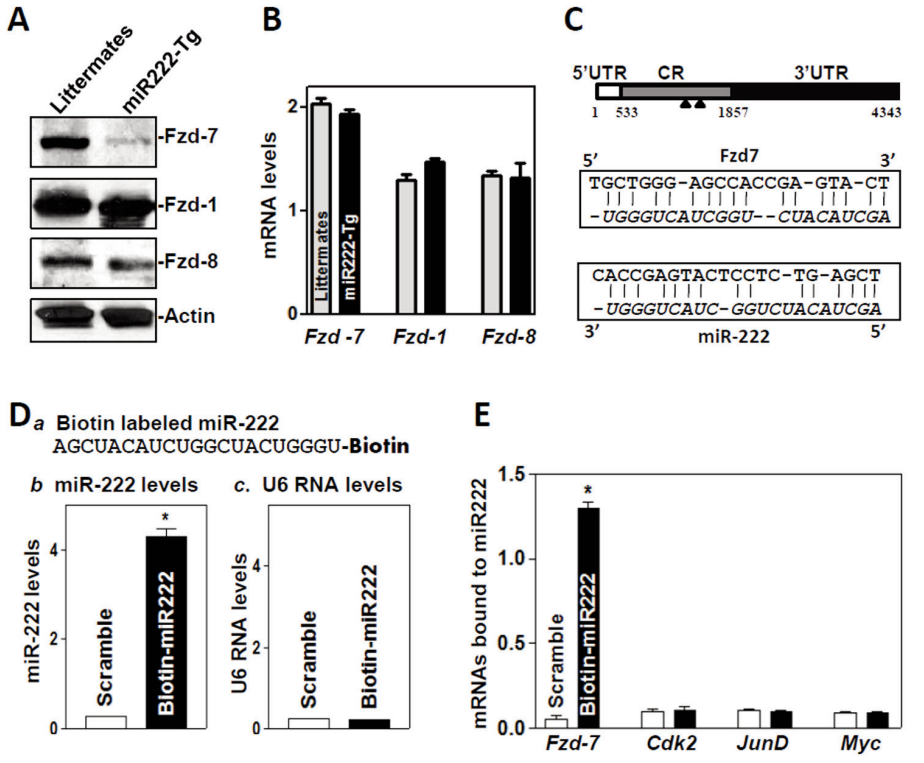

Figure 5. miR-222 directly interacts with the *Fzd7* mRNA. (A) Immunoblots of FZD proteins in the small intestinal mucosa. (B) *Fzd* mRNA levels in the mucosa. Values are the mean ± SEM (n = 5). (C) Schematic representation of *Fzd7* mRNA depicting predicted target sites for miR-222 in its coding region (CR). (D) miR-222 and U6 levels in IEC-6 cells transfected with biotinylated miR-222 for 24 h. Values are mean ± SEM (n = 3). *$P < 0.05$ compared with cells transfected with scramble. (E) Levels of *Fzd7, Cdk2, JunD* and *Myc* mRNAs in the materials pulled down by biotin-miR-222.

sized FZD7 protein decreased significantly in pre-miR-222 transfected cells compared with cells transfected with scrambled oligomer. Inhibition of FZD7 protein synthesis by miR-222 was relatively specific, since miR-222 overexpression did not alter the rate of nascent GAPDH synthesis. To further define the role of miR-222 in FZD7 translation, we examined the relative distribution of the *Fzd7* mRNA in individual fractions from polyribosome gradients after miR-222 overexpression. Although increasing the levels of miR-222 did not affect global polysomal profiles (data not shown), the abundance of the *Fzd7* mRNA associated with actively translating fractions (fractions 7–9) decreased remarkably in pre-miR-222–transfected cells with a significant shift of *Fzd7* mRNA to low-translating fractions (fractions 5 and 6; Figure 6D, top). In contrast, *Gapdh* mRNA, encoding the housekeeping protein GAPDH, distributed similarly in both groups (Figure 6D, bottom). To determine if the inhibition by miR-222 was mediated through the *Fzd7* CR or 3′-UTR, fractions of the *Fzd7* CR and 3′-UTR were subcloned into the pmirGLO dual-luciferase miRNA target expression vector to generate pmirGLO-Fzd7-CR and pmirGLO-Fzd7-3′-UTR reporter constructs (Figure 6E, schematic). As shown, miR-222 overexpression decreased the levels of Fzd7-CR luciferase reporter activity, but it failed to inhibit the activities of Fzd7-3′-UTR reporters (Figure 6E, right). We also examined FZD7 levels in miR-222–silenced cells and demonstrated that decreasing the levels of miR-222 by transfection with anti-miR-222 oligomer increased FZD7 protein levels but had no effect on *Fzd7* mRNA content (Supplementary Figure S5). These results indicate that miR-222 interacts with the *Fzd7* mRNA via its CR, thus repressing FZD7 translation.

MiR-222–Modulated FZD7 Plays a Critical Role in Intestinal Epithelial Repair

This study used an *in vitro* epithelial repair model, in which IEC-6 cells were cocultured with Wnt overexpressing fibroblasts as described previously (29). Because FZD7 is the receptor of Wnt5a signaling (30,31), IEC-6 cells were cocultured with stable Wnt5a-Fs. Coculture of IEC-6 cells with Wnt5a-Fs significantly enhanced epithelial repair after wounding, although parental fibroblasts (Con-Fs) cocultured IEC-6 cells did not alter the wound repair (Supplementary Figure S6). Interestingly, increasing the levels of miR-222 by pre-miR-222 transfection inhibited this stimulation induced by Wnt5a-Fs cocultured with IEC-6 cells (Figures 7A, B). The wounded area was almost completely covered 16 h after wounding when cells were transfected with scramble, but it was only healed by ~40% in cells transfected with pre-miR-222. FZD7 silencing by transfection with siRNA targeting *Fzd7* mRNA (siFzd7) had a similar inhibitory effect on epithelial repair (Figures 7C, D). Results in Figure 7E further showed that Wnt-dependent transcriptional activity increased significantly after wounding, but this induction was prevented by miR-222 overexpression or FZD7 silencing. When IEC-6 cells were cultured alone, increasing the levels of miR-222 also repressed epithelial repair, but the inhibition was weak compared with that observed in the coculture model (Supplementary Figure S7). In addition, neither pre-miR-222 nor siFzd7 affected cell viability as measured by Trypan blue staining (data not shown). Together, these findings indicate that miR-222 represses epithelial repair after wounding primarily by inactivating Wnt signals through downregulation of FZD7 expression.

DISCUSSION

Our previous studies demonstrated that inhibition of IEC-6 cell proliferation by polyamine depletion is associated with increased miR-222 expression, whereas miR-222 silencing enhances cell division (3,12). However, this study was conducted in cultured IECs, and miR-222 has been considered to act as a tumor suppressor or oncogene in cancer development (12,21–23); therefore, the exact function of miR-222 in the intestinal epithelium *in vivo* remains to be fully investigated. By using a tissue-specific transgenic expression approach, here we provided powerful genetic evidence that miR-222 plays an important role in the regulation of intestinal mucosal regeneration and protection. Transgene-driven overexpression of miR-222 in IECs caused small intestinal mucosal atrophy, delayed epithelial repair after I/R-induced injury and aggravated the barrier dysfunction in mice exposed to CLP. The miR-222–overexpressing epithelium also exhibited decreased expression of the Wnt receptor FZD7; miR-222 was found to directly interact with and repress *Fzd-7* mRNA translation. These findings advance our understanding of the physiological function of miR-222 in maintenance of the intestinal epithelial integrity and highlight the involvement of increased miR-222 in gut mucosal pathology.

The results reported here are the first demonstration that miR-222 functions as a biological repressor of normal mucosal growth in the small intestine. As shown, miR222-Tg mice exhibited a significant inhibition of mucosal growth, as evidenced by a decrease in cell proliferation in the crypts and subsequent shrinkage of crypts and villi in the mucosal tissue. These observations from *in vivo* studies are consistent with the findings obtained from our previous *in vitro* cell biology studies that ectopic overexpression of miR-222 precursors in cultured IEC-6 cells inhibits *Cdk4* mRNA translation, thus causing G1 phase growth arrest (12). This inhibitory phenotype in mucosal growth by miR-222 occurs only in the

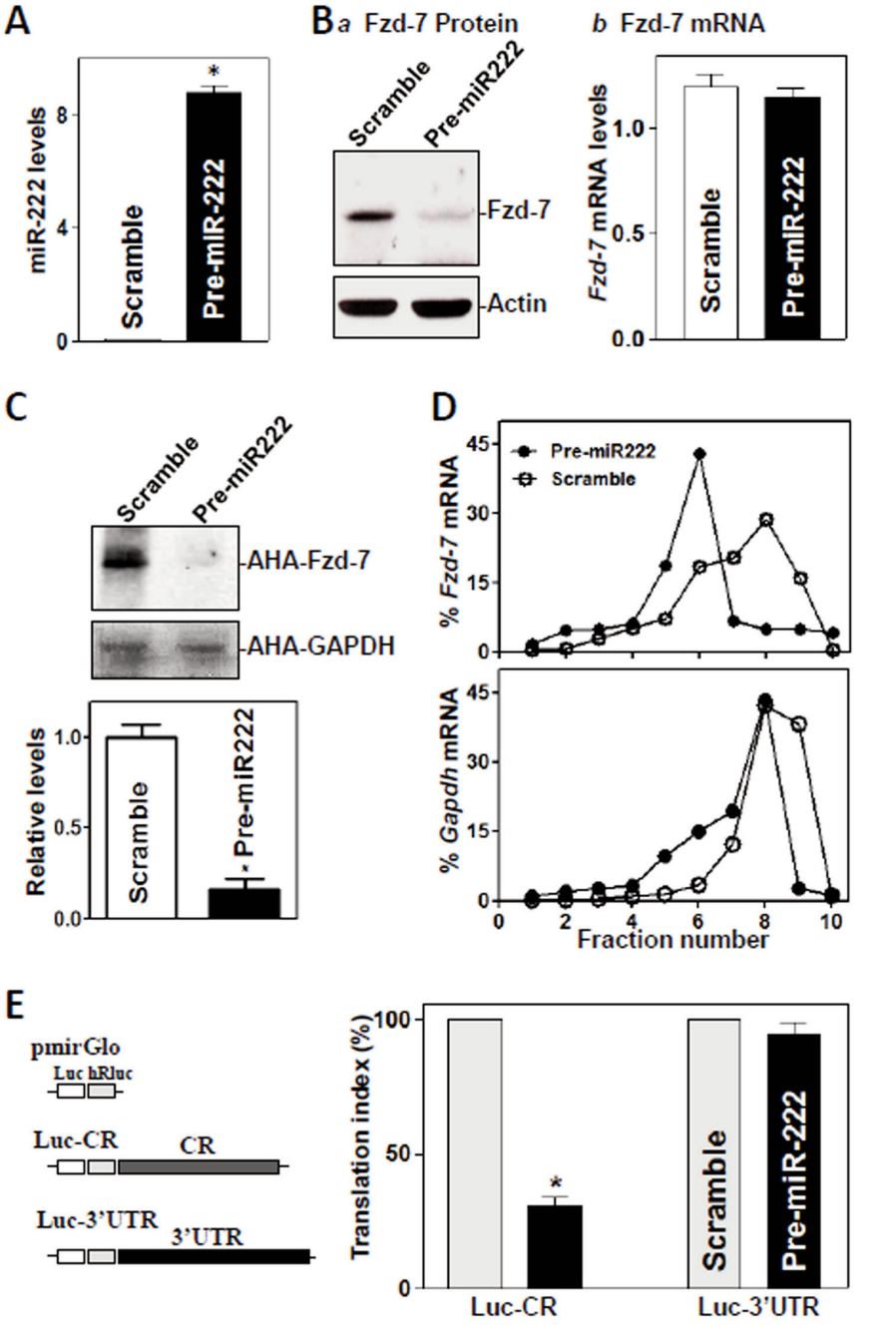

Figure 6. miR-222 represses FZD7 translation. (A) miR-222 levels 48 h after transfection with pre-miR-222. Values are mean ± SEM (n = 3). **P* < 0.05 compared with scramble. (B) Immunoblots of FZD7 protein (a) and its mRNA as measured by Q-PCR analysis (b) in cells described in (A). (C) Newly synthesized FZD7 protein as measured by L-azidohomoalaine (AHA) kit. Top, representative immunoblots of newly synthesized FZD-7; bottom, quantitative analysis of the immunoblotting signals as measured by densitometry. Values are mean ± SEM of data from three separate experiments. (D) Distributions of *Fzd7* (top) and *Gapdh* (bottom) mRNAs in each gradient fraction. Nuclei were pelleted, and the resulting supernatants were fractionated through a 10–50% linear sucrose gradient. The levels of *Fzd7* and *Gapdh* mRNAs were plotted as a percentage of the total *Fzd7* or *Gapdh* mRNA levels in the samples. (E) Levels of reporter activities (n = 6).

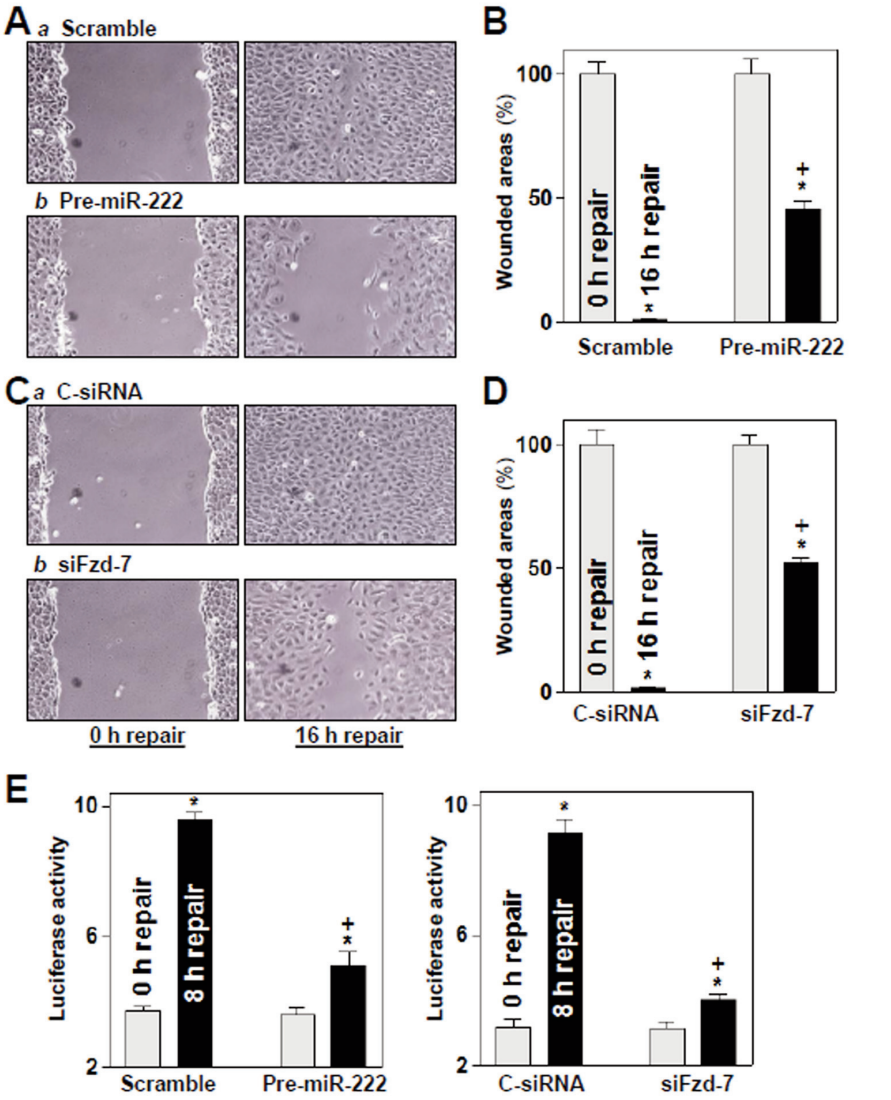

Figure 7. miR-222 inhibits epithelial repair in IEC-6 cells cocultured with Wnt5a-transfected fibroblasts after wounding. (A) Imaging pictures of epithelial repair: scramble (a) and cells (b) transfected with pre-miR-222 for 48 h. The monolayer was wounded, and plates were photographed immediately or 16 h thereafter. (B) Summarized data in cells described in (A). Values are the mean ± SEM (n = 6). $^{*,+}P < 0.05$ compared with 0 h repair and 16 h repair of scramble-transfected cells, respectively. (C) Epithelial repair 48 h after silencing FZD7: (a) C-siRNA transfection and (b) siFzd7 transfection. (D) Summarized data from cells described in (C). (E) Changes in Wnt-dependent transcription activity as measured by pMyc-TA-luciferase reporter gene assays 8 h after wounding with or without transfection with pre-miR-222 (left) or siFzd7 (right).

small intestine, since there were no differences in the rates of colonic mucosal growth between miR222-Tg mice and littermates, although miR-222 levels in the colonic mucosa were also increased in miR222-Tg mice. The exact reasons for which miR-222 overexpression failed to alter colonic mucosal growth remain unknown, but basal mucosal turnover rate in the colon is lower than that observed in the small intestine (32). Consistent with this finding, we recently reported that targeted deletion of the RBP HuR in IECs causes mucosal growth inhibition in the small intestine but not in the colon (33). The miR-222–elevated epithelium also displayed the impaired mucosal maturation and increased susceptibility to TNFα-induced apoptosis in the small intestine, and these changes may also contribute to disruption of the intestinal epithelial integrity in miR222-Tg mice. On the other hand, inhibition of miR-222 by the simple systemic delivery of locked nucleic acid-modified antimiR-222 was found to block exercise-induced cardiac growth in mice (43). Interestingly, basal rates of cardiac growth and cardiomyocyte proliferation are also slow under biological conditions.

Another significant finding from this study is that the miR-222–overexpressing intestinal epithelium exhibits an increased vulnerability to pathological stress. Increased levels of miR-222 in the intestinal epithelium not only delayed mucosal repair after I/R-induced injury but also exacerbated the gut barrier dysfunction in mice exposed to CLP. The inhibitory effect of miR-222 on mucosal repair is not surprising, because miR-222 modulates expression of several migration-associated (34) and proliferation-promoting proteins (12,35,36) that are essential for rapid epithelial restitution and chronic mucosal healing after injury (37). This notion is further supported by our *in vitro* studies showing that elevation of miR-222 in cultured IEC-6 cells repressed epithelial repair after wounding. On the other hand, transgenic miR-222 expression deteriorated the gut barrier dysfunction in CLP mice by downregulating expression of TJ proteins, since miR-222–overexpressing epithelium displayed an additional decrease in the levels of claudin-1 and ZO-1 after exposure to CLP. The TJ proteins are the apical-most element of the junctional complex and seal epithelial cells together in a way that prevents even small molecules from leaking between cells (10,38). TJs are highly dynamic, and their constituent protein complexes undergo continuous remodeling and turnover under tight regulation by numerous extracellular and intracellular

factors. Maintenance of dynamic levels of TJ proteins is critical for normal function of the epithelial barrier, whereas disruption of TJ expression results in acute gut barrier dysfunction. However, it remains unknown at present whether miR-222 directly targets the TJ mRNAs or regulates TJ expression indirectly.

The results presented here also show that *Fzd7* mRNA is a novel target of miR-222 and that [miR-222/*Fzd7* mRNA] association represses FZD7 translation. The expression level of FZD7 protein in miR-222–elevated intestinal epithelium decreased dramatically, although there was no change in total *Fzd7* mRNA content in miR222-Tg mice. Studies using biotin-labeled miR-222 demonstrated that miR-222 directly bound *Fzd7* mRNA but not *Cdk2*, *JunD* or *Myc* mRNAs in IEC-6 cells. Through the use of various ectopic reporters bearing partial transcripts spanning the *Fzd7* CR and 3′-UTR with or without miR-222–binding sites, our results further show that miR-222 interacted predominantly with the *Fzd7* CR but not with the *Fzd7* 3′-UTR. These findings are consistent with other results that miR-222 associates with the mRNAs such as *MMP1* and *SOD2* (34), p27kip1 (35), *eNOS* (18), *LASS2* (19), *PPP2R2A* (40), *TIMP3* (38), ER-α (23) and *CD4* (17), thus destabilizing mRNAs and/or repressing their translation. Generally, miR-222 interacts with the 3′-UTRs of target transcripts, although, in some instances, it also associates with the CR or 5′-UTR of target mRNAs for its regulatory actions. In this regard, we have reported that miR-222 represses *Cdk4* mRNA translation by interacting with the *Cdk4* CR rather than the 3′-UTR (12).

Intestinal epithelium-specific transgenic expression of miR-222 inhibits small intestinal mucosal growth and delays repair of damaged mucosa at least partially by inactivating Wnt signaling as a result of repression of FZD7 expression. Wnt signaling is crucial for gut development and acts as a key regulator of normal epithelial renewal and mucosal repair after injury (30,31). In response to stress, released Wnt proteins in the extracellular milieu bind to serpentine receptors of the FZD family, which leads to an accumulation of dephosphorylated β-catenin and its stabilization (30). Subsequently, the stabilized β-catenin undergoes nuclear translocation and association with TCF transcription factors, enabling transactivation of their target genes. Target deletion of conditional *Wnt* gene or overexpression of the Wnt natural inhibitor, Dickkopf1, disrupts gut development, represses mucosal growth and delays healing after injury (41,42). Consistent with our previous studies (29), coculture of IECs with Wnt-overexpressing fibroblasts enhanced epithelial repair, but this stimulation was prevented by miR-222 overexpression. Moreover, FZD7 levels decreased dramatically in the intestinal mucosal tissue in miR222-Tg mice and in the miR-222–overexpressing population of IEC-6 cells. FZD7 silencing or decreased levels of FZD7 by miR-222 overexpression inhibited Wnt-dependent transcriptional activity and repressed epithelial repair in the presence of Wnt5a.

CONCLUSION

These findings indicate that miR-222 functions as a negative regulator of intestinal epithelium homeostasis by altering Wnt signaling activity through posttranscriptional regulation of FZD7 expression.

ACKNOWLEDGMENTS

Funding was provided by Merit Review Awards (to JY Wang, DJ Turner and JN Rao) from the U.S. Department of Veterans Affairs; grants from the National Institutes of Health (DK57819, DK61972 and DK68491 to JY Wang); and the National Institute on Aging–Intramural Research Program (to M Gorospe). JY Wang is a Senior Research Career Scientist, Biomedical Laboratory Research and Development Service, U.S. Department of Veterans Affairs.

DISCLOSURE

The authors declare that they have no competing interests as defined by *Molecular Medicine*, or other interests that might be perceived to influence the results and discussion reported in this paper.

REFERENCES

1. Sato T, Clevers H. (2013) Growing self-organizing mini-guts from a single intestinal stem cell: mechanism and applications. *Science.* 340:1190–4.
2. Günther C, Neumann H, Neurath MF, Becker C. (2013) Apoptosis, necrosis and necroptosis: cell death regulation in the intestinal epithelium. *Gut.* 62:1062–71.
3. Xiao L, Wang JY. (2014) RNA-binding proteins and microRNAs in gastrointestinal epithelial homeostasis and diseases. *Curr. Opin. Pharmacol.* 19:46–53.
4. Puleo F, Arvanitakis M, Van Gossumm A, Preiser JC. (2011) Gut failure in the ICU. *Semin. Respir. Crit. Care Med.* 32:626–38.
5. Carter SR, *et al.* (2013) Intestinal barrier disruption as a cause of mortality in combined radiation and burn injury. *Shock.* 40:281–9.
6. Mendell JT, Olson EN. (2012) MicroRNAs in stress signaling and human disease. *Cell.* 148:1172–87.
7. Omer AD, Janas MM, Novina CD. (2009) The chicken or the egg: microRNA-mediated regulation of mRNA translation or mRNA stability. *Mol. Cell* 35:739–40.
8. Eulalio A, Huntzinger E, Izaurralde E. (2008) Getting to the root of miRNA-mediated gene silencing. *Cell.* 132:9–14.
9. Leung AK, Sharp PA. (2010) MicroRNA functions in stress responses. *Mol. Cell.* 40:205–15.
10. Yang H, Rao JN, Wang JY. (2014) Posttranscriptional regulation of intestinal epithelial tight junction barrier by RNA-binding proteins and microRNAs. *Tissue Barriers.* 2:e28320.
11. Ouyang M, *et al.* (2015) Modulation by miR-29b of intestinal epithelium homoeostasis through the repression of menin translation. *Biochem. J.* 465:315–23.
12. Xiao L, *et al.* (2011) Regulation of cyclin-dependent kinase 4 translation through CUG-binding protein 1 and microRNA-222 by polyamines. *Mol. Biol. Cell* 22:3055–69.
13. Xiao L, *et al.* (2013) miR-29b represses intestinal mucosal growth by inhibiting translation of cyclin-dependent kinase 2. *Mol. Biol. Cell.* 24:3038–46.
14. Cao S, *et al.* (2014) Inhibition of Smurf2 translation by miR-322/503 modulates TGF-β/Smad2 signaling and intestinal epithelial homeostasis. *Mol. Biol. Cell.* 25:1234–43.
15. Zhuang R, *et al.* (2013) miR-195 competes with HuR to modulate stim1 mRNA stability and regulate cell migration. *Nucleic Acids Res.* 41:7905–19.
16. Galardi S, *et al.* (2007) miR-221 and miR-222 expression affects the proliferation potential of human prostate carcinoma cell lines by targeting $p27^{Kip1}$. *J. Biol. Chem.* 282:23716–24.
17. Orecchini E, *et al.* (2014) The HIV-1 Tat protein modulates CD4 expression in human T cells through the induction of miR-222. *RNA Biol.* 11:334–8.
18. Evangelista AM, Deschamps AM, Liu D, Raghavachari N, Murphy E. (2013) miR-222 contributes to sex-dimorphic cardiac eNOS expression via ets-1. *Physiol. Genomics* 45:493–8.

19. Yu B, *et al.* (2012). miR-221 and miR-222 promote Schwann cell proliferation and migration by targeting LASS2 after sciatic nerve injury. *J. Cell Sci.* 125:2675–83.
20. Garofalo M, Quintavalle C, Romano G, Croce CM, Condorelli G. (2012) miR-221/222 in cancer: their role in tumor progression and response to therapy. *Curr. Mol. Med.* 12:27–33.
21. Yamashita R, *et al.* (2015) Growth inhibitory effects of miR-221 and miR-222 in non-small cell lung cancer cells. *Cancer Med.* 4:551–64.
22. Liu S, *et al.* (2014) A microRNA 221- and 222-mediated feedback loop maintains constitutive activation of NFκB and STAT3 in colorectal cancer cells. *Gastroenterology.* 147:847–59.
23. Shi Z, *et al.* (2014) Differential expression of microRNAs in omental adipose tissue from gestational diabetes mellitus subjects reveals miR-222 as a regulator of ERα expression in estrogen-induced insulin resistance. *Endocrinology.* 155:1982–90.
24. Cafferata EG, *et al.* (2009) A novel A33 promoter-based conditionally replicative adenovirus suppresses tumor growth and eradicates hepatic metastases in human colon cancer models. *Clin. Cancer Res.* 15:3037–49.
25. Flentjar N, *et al.* (2007) TGF-βRII rescues development of small intestinal epithelial cells in Elf3-deficient mice. *Gastroenterology.* 132:1410–9.
26. Hart ML, *et al.* (2011) Hypoxia-inducible factor-1α-dependent protection from intestinal ischemia/reperfusion injury involves ecto-5′-nucleotidase (CD73) and the A2B adenosine receptor. *J. Immunol.* 186:4367–74.
27. Wang JY, Johnson LR. (1992) Luminal polyamines substitute for tissue polyamines in duodenal mucosal repair after stress in rats. *Gastroenterology.* 102:1109–17.
28. Yu TX, *et al.* (2011) Chk2-dependent HuR phosphorylation regulates occludin mRNA translation and epithelial barrier function. *Nucleic Acids Res.* 39:8472–87.
29. Liu L, *et al.* (2012) Activation of Wnt3a signaling stimulates intestinal epithelial repair by promoting c-Myc-regulated gene expression. *Am. J. Physiol. Cell Physiol.* 302:C277–85.
30. Clevers H. (2006) Wnt/β-catenin signaling in development and disease. *Cell.* 127:469–80.
31. Krausova M, Korinek V. (2014) Wnt signaling in adult intestinal stem cells and cancer. *Cell Signal.* 26:570–9.
32. Johnson LR. (1988) Regulation of gastrointestinal mucosal growth. *Physiol. Rev.* 68:456–502.
33. Liu L, *et al.* (2014) RNA-binding protein HuR promotes growth of small intestinal mucosa by activating the Wnt signaling pathway. *Mol. Biol. Cell.* 25:3308–18.
34. Liu X, *et al.* (2009) MicroRNA-222 regulates cell invasion by targeting matrix metalloproteinase 1 (MMP1) and manganese superoxide dismutase 2 (SOD2) in tongue squamous cell carcinoma cell lines. *Cancer Genomics Proteomics.* 6:131–9.
35. le Sage C, *et al.* (2007) Regulation of the $p27^{Kip1}$ tumor suppressor by miR-221 and miR-222 promotes cancer cell proliferation. *EMBO J.* 26:3699–708.
36. Felli N, *et al.* (2005) MicroRNAs 221 and 222 inhibit normal erythropoiesis and erythroleukemic cell growth via kit receptor down-modulation. *Proc. Natl. Acad. Sci. U. S. A.* 102:18081–6.
37. Gao JH, Guo LJ, Huang ZY, Rao JN, Tang CW. (2013) Roles of cellular polyamines in mucosal healing in the gastrointestinal tract. *J. Physiol. Pharmacol.* 64:681–93.
38. Odenwald MA, Turner JR. (2013) Intestinal permeability defects: is it time to treat? *Clin. Gastroenterol. Hepatol.* 11:1075–83.
39. Zhou S, *et al.* (2015) MiR-21 and miR-222 inhibit apoptosis of adult dorsal root ganglion neurons by repressing TIMP3 following sciatic nerve injury. *Neurosci. Lett.* 586:43–9.
40. Dong R, *et al.* (2015) miR-222 overexpression may contribute to liver fibrosis in biliary atresia by targeting PPP2R2A. *J. Pediatr. Gastroenterol. Nutr.* 60:84–90.
41. van Es JH, *et al.* (2005) Wnt signalling induces maturation of Paneth cells in intestinal crypts. *Nat. Cell Biol.* 7:381–6.
42. Koch S, *et al.* (2009) Dkk-1 inhibits intestinal epithelial cell migration by attenuating directional polarization of leading edge cells. *Mol. Biol. Cell.* 20:4816–25.
43. Liu X, *et al.* (2015) miR-222 is necessary for exercise-induced cardiac growth and protects against pathological cardiac remodeling. *Cell Metab.* 21:584–95.

Cite this article as: Chung HK, *et al.* (2015) Transgenic expression of miR-222 disrupts intestinal epithelial regeneration by targeting multiple genes including Frizzled-7. *Mol. Med.* 21:676–87.